Journal of Marine Systems xxx (2008) xxx–xxx

Contents lists available at ScienceDirect

Journal of Marine Systems

journal homepage: www.elsevier.com/locate/jmarsys

Skill assessment of a spectral ocean–atmosphere radiative model

Watson W. Gregg [a,*], Nancy W. Casey [b]

[a] Global Modeling and Assimilation Office, NASA/Goddard Space Flight Center, Greenbelt, MD 20771, United States
[b] Science Systems and Applications, Inc., Lanham, MD 20706, United States

ARTICLE INFO

Article history:
Received 30 March 2007
Received in revised form 27 December 2007
Accepted 2 May 2008
Available online xxxx

Keywords:
Radiative transfer
Ocean ecosystems
Surface irradiance
Spectral irradiance
Shortwave radiation
Primary production

ABSTRACT

Ocean phytoplankton, detrital material, and water absorb and scatter light spectrally. The Ocean–Atmosphere Spectral Irradiance Model (OASIM) is intended to provide surface irradiance over the oceans with sufficient spectral resolution to support ocean ecology, biogeochemistry, and heat exchange investigations, and of sufficient duration to support inter-annual and decadal investigations. OASIM total surface irradiance (integrated 200 nm to 4 μm) was compared to in situ data and three publicly available global data products at monthly 1-degree resolution.
OASIM spectrally-integrated surface irradiance had root mean square (RMS) difference = 20.1 W m^{-2} (about 11%), bias = 1.6 W m^{-2} (about 0.8%), regression slope = 1.01 and correlation coefficient = 0.89, when compared to 2322 in situ observations. OASIM had the lowest bias of any of the global data products evaluated (ISCCP-FD, NCEP, and ISLSCP II), and the best slope (nearest to unity). It had the second best RMS, and the third best correlation coefficient. OASIM total surface irradiance compared well with ISCCP-FD (RMS = 20.7 W m^{-2}; bias = −11.4 W m^{-2}, r = 0.98) and ISLSCP II (RMS = 25.2 W m^{-2}; bias = −13.8 W m^{-2}; r = 0.97), but less well with NCEP (RMS = 43.0 W m^{-2}; bias = −22.6 W m^{-2}; r = 0.91). Comparisons of OASIM photosynthetically available radiation (PAR) with PAR derived from SeaWiFS showed low bias (−1.8 mol photons m^{-2} d^{-1}, or about 5%), RMS (4.25 mol photons m^{-2} d^{-1}, or about 12%), near unity slope (1.03) and high correlation coefficient (0.97). Coupled with previous estimates of clear sky spectral irradiance in OASIM (6.6% RMS at 1 nm resolution), these results suggest that OASIM provides reasonable estimates of surface broadband and spectral irradiance in the oceans, and can support studies on ocean ecosystems, carbon cycling, and heat exchange.

Published by Elsevier B.V.

1. Introduction

When light enters the ocean from the atmosphere, it initiates a series of events that leads to the existence of nearly all marine life. The first event in this sequence is photosynthesis, where ocean phytoplankton absorb light and convert it to organic carbon. Light, or irradiance, entering the ocean is thus critical for marine photosynthesis, ecosystems, fisheries, and carbon dynamics. Additionally, the irradiance absorbed by the ocean plays a critical role in the temperature of the ocean, contributes to the vertical density structure and surface ocean photochemistry, and affects the exchange of heat with the atmosphere. Models and algorithms simulating these processes require realistic representations of irradiance entering the oceans. This begins with irradiance propagation through the atmosphere and into the ocean surface.

There are many radiative transfer models of the atmosphere (e.g., see recent comparison by Halthore et al., 2005), most of which are applicable over the oceans. These range spectrally from line-by-line models at 1-nm resolution (Yang et al., 1999) to broadband representations of about 100 μm (see Halthore et al., 2005). The high spectral resolution models come with a complexity unnecessary for most biological/physical/photochemical applications and with a prohibitive run-time cost. The broadband models contain insufficient spectral resolution necessary for many ocean biological applications.

There are also several publicly available global data products of surface irradiance. These include International Satellite Cloud Climatology Project (ISCCP-FD; Zhang et al.,

* Corresponding author.
E-mail addresses: watson.gregg@nasa.gov (W.W. Gregg), ncasey@gmao.gsfc.nasa.gov (N.W. Casey).

0924-7963/$ – see front matter. Published by Elsevier B.V.
doi:10.1016/j.jmarsys.2008.05.007

2004), National Center for Environmental Prediction (NCEP) Reanalysis (Kalnay et al., 1996), and International Satellite Land Surface-Climatology Project (ISLSCP II; Hall et al., 2005). These irradiance data products are integrated over the entire solar spectrum. Ocean phytoplankton do not absorb energy over the entire solar spectrum. Rather, they absorb predominantly in the visible wavelengths, and selectively at that. This is true also for seawater absorption and scattering as well as photochemical reactions such as those related to chromophoric dissolved organic matter (CDOM) (Fig. 1). Consequently, these broadband data products have limited usefulness for ocean ecosystem, carbon dynamics, and photochemistry research, as well as heat exchange and ocean general circulation.

Photosynthetically available radiation (PAR) is a subset of total solar irradiance (350–700 nm). A data product derived from the Sea-viewing Wide Field-of-view Sensor (SeaWiFS) is also publicly available. This product is much more useful for ocean ecosystems studies (less so for heat exchange applications), but again phytoplankton absorb selectively even within the PAR spectral range.

It is also desirable that a model spans enough time to permit investigations of inter-annual and decadal variability. Thorough, quantitative assessment of the skill of such a model is required to promote its realism and usefulness for oceanic studies.

Here we present the Ocean–Atmosphere Spectral Irradiance Model (OASIM), which is intended to provide surface irradiance representations over the oceans with sufficient spectral resolution to support ocean ecology, biogeochemistry, and heat exchange investigations, and of sufficient duration to support inter-annual and decadal investigations. OASIM is tailored specifically for biological applications, with minimal complexity while achieving necessary resolution, at reasonable computational expense. It is used routinely in coupled physical–biological simulations of the global oceans (e.g., Gregg et al., 2003; Carr et al., 2006; Gregg and Casey, 2007) over multi–year and decadal time scales without excessive computational burden.

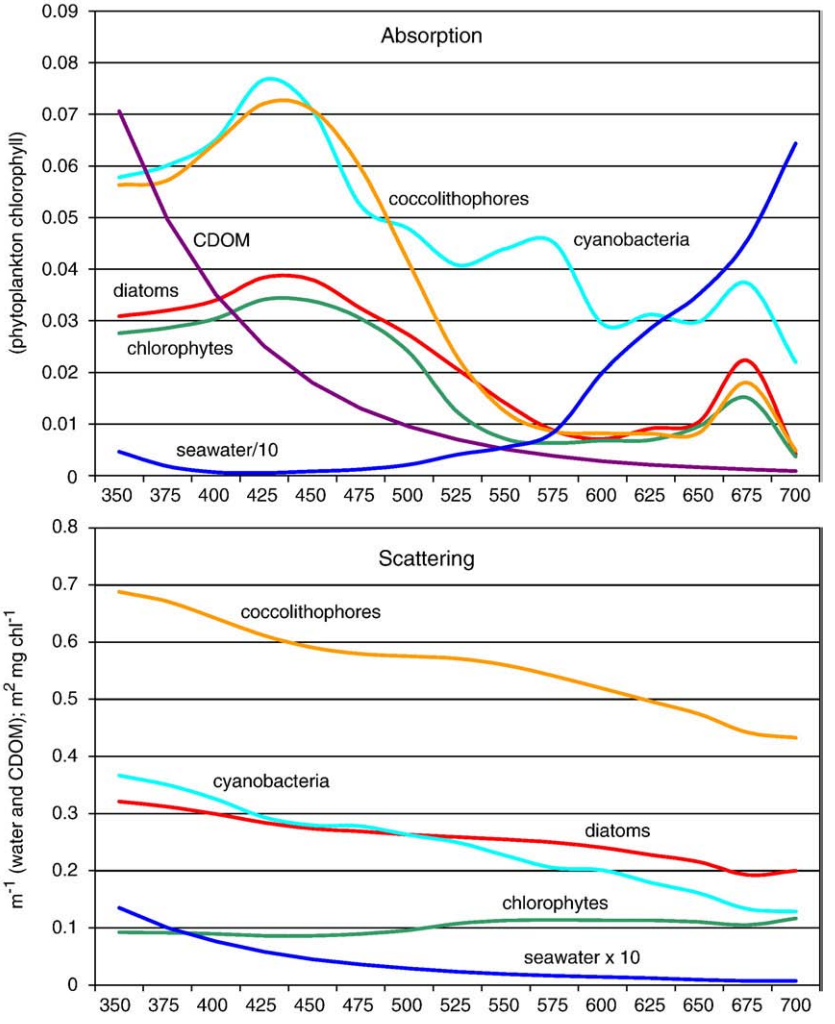

Fig. 1. Spectral absorption and scattering coefficients of common phytoplankton groups, CDOM, and water. Water absorption data are from Smith and Baker (1981) for 200–370 nm and 730–800 nm, Pope and Fry (1997) for 280–720 nm, Circio and Petty (1951) for 800 nm–1.5 μm, and Maul (1985) for 2.5–4 μm. Phytoplankton group-specific optical properties are derived from laboratory observations (Morel and Bricaud, 1981; Bricaud et al., 1983, 1988; Sathyendranath et al., 1987; Morel, 1988; Ahn et al., 1992).

Please cite this article as: Gregg, W.W., Casey, N.W., Skill assessment of a spectral ocean–atmosphere radiative model, Journal of Marine Systems (2008), doi:10.1016/j.jmarsys.2008.05.007

OASIM follows the development by Bouvet et al. (2002) in that it extends the Gregg and Carder (1990) model to incorporate clouds, and derives atmospheric optical properties from satellite observations. However, OASIM uses an explicit spectral formulation for cloud radiative transfer, found by Bartlett et al. (1998) and Siegel et al. (1999) to be important. Additionally, OASIM extends the spectral domain (from 200 nm to 4 μm) to support studies on ocean heat exchange and the temporal domain (1979–2005) to support studies involving long-term changes and variability.

The primary advantage of OASIM over other models and data products for ocean biological and photochemical research is its spectral nature. However, data sets for skill assessment are quite limited in spatial, temporal, and spectral availability. As an intermediate step in the skill assessment of OASIM, we utilize data products and sets of broadband observations, which are distributed globally and over decades. While not satisfying the requirement of a complete assessment of OASIM, when coupled with previous limited spectral evaluations, this broadband evaluation can provide additional insight into the capability of this model for use in ocean biological, chemical, and physical applications.

2. Model

OASIM is based on the Gregg and Carder (1990) spectral model for clear skies, and Slingo (1989) for spectral cloud transmittance. The clear and cloudy sky models track two irradiance streams to the ocean surface: direct and diffuse (Fig. 2), which are defined mathematically by

$$E_d(\lambda) = F_o(\lambda)\cos\theta T_g(\lambda)[(1-\mathrm{cov}/100)T_{dclr}(\lambda) + (\mathrm{cov}/100)T_{dcld}(\lambda)][1-\rho_d(\lambda)] \quad (1)$$

$$E_s(\lambda) = F_o(\lambda)\cos\theta T_g(\lambda)[(1-\mathrm{cov}/100)T_{sclr}(\lambda) + (\mathrm{cov}/100)T_{scld}(\lambda)][1-\rho_s(\lambda)] \quad (2)$$

where symbols and definitions are shown in Table 1. The subscript cld indicates cloudy skies, and clr indicates clear skies.

The terms containing the subscript clr in each of Eqs. (1) and (2) represents the clear sky irradiance impinging on the ocean surface, and the term with cld represents the cloudy sky irradiance. Both the clear and cloudy sky irradiances are transmitted across the ocean interface by the reflectance terms $[1-\rho_{d,s}(\lambda)]$.

The clear sky model of Gregg and Carder (1990) was derived from Bird and Riordan (1986), but was limited to the spectral range of PAR, defined here as 350–700 nm. It also contained high spectral resolution (1 nm). This model is extended for OASIM to the entire solar spectrum, 200 nm to 4 μm, representing >99% of the total solar irradiance impinging on the top of the atmosphere. To reduce the computational load for global applications, the spectral resolution is degraded from Gregg and Carder (1990) to a variable resolution appropriate for the spectral absorbing properties of the major atmospheric optically active gases, specifically ozone, water vapor, oxygen, and carbon dioxide (Table 2). The spectral resolution is fixed at 25 nm for the PAR range, which is the region of interest for phytoplankton photosynthesis. There are 33 bands in OASIM across the entire spectrum.

Extraterrestrial solar irradiance, Rayleigh optical thickness, and absorption coefficients for atmospheric gases are also shown for the OASIM spectral bands in Table 2. Extraterrestrial irradiance was taken from Thekaekara (1974) for the spectral range 200–330 nm, Neckel and Labs (1984) for 330 nm–1.25 μm, and Tanre et al. (1990) for 1.25–4 μm. Rayleigh optical thickness was from Bird and Riordan (1986), ozone absorption coefficients from Inn and Tanaka (1953), and coefficients for the other gases from Tanre et al. (1990).

A modification to the Gregg and Carder (1990) clear sky model is the use of aerosol distributions and characteristics derived from global satellite observations. Previously aerosols were parameterized as a function of wind speed, relative humidity, and visibility. This characterization was only applicable for marine (sea salt) aerosols.

Aerosol information from the Moderate Resolution Imaging Spectroradiometer (MODIS), including aerosol $\tau_a(\lambda)$, $\omega_a(\lambda)$, and $\alpha(\lambda)$ (see Table 1 for definitions) are available at 7 wavelengths, 470, 550, 660, 870 nm, and 1.24, 1.64, and 2.13 μm (Remer et al., 2005). Between 470 nm and 2.13 μm, we use a cubic spline interpolation to convert to OASIM wavelengths. Shorter than 470 nm, we linearly extrapolate from the 470–550 nm wavelength pair. We extrapolate similarly for OASIM wavelengths >2.13 μm, using the slope derived from the MODIS 1.64–2.13 μm pair. OASIM requires the forward scattering probability, which can be calculated from the MODIS asymmetry parameter using Bird and Riordan (1986):

$$F_a = 1-0.5\exp[(A + B\cos\theta)\cos\theta] \quad (3)$$

$$A = C[1.459 + C(0.1595 + C0.4129)] \quad (4)$$

$$B = C[0.0783 + C(-0.3824-C0.5874)] \quad (5)$$

$$C = \ln(1-\alpha) \quad (6)$$

where wavelength-dependence has been dropped.

MODIS aerosol data are only available since Feb 2000. Prior to this date, we use aerosol optical thickness data from the Advanced Very High Resolution Radiometer (AVHRR) series (Stowe et al., 2002).

AVHRR τ_a is available at only one wavelength, 630 nm. To obtain spectral $\tau_a(\lambda)$ information from the AVHRR, we first

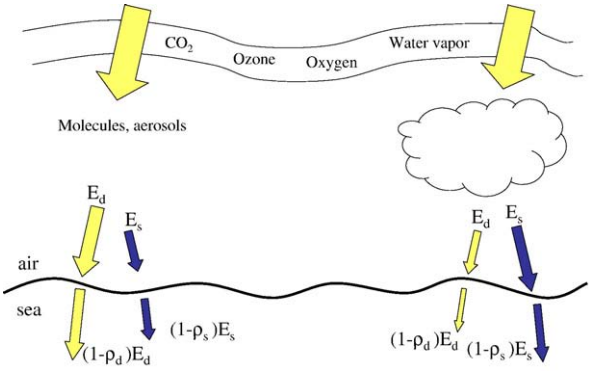

Fig. 2. Irradiance pathways in OASIM for clear skies (left) and cloudy skies (right). E_d is direct downwelling irradiance, E_s is diffuse downwelling, and ρ_d and ρ_s are direct and diffuse surface reflectances. All irradiances and reflectances are spectrally-resolved.

Please cite this article as: Gregg, W.W., Casey, N.W., Skill assessment of a spectral ocean–atmosphere radiative model, Journal of Marine Systems (2008), doi:10.1016/j.jmarsys.2008.05.007

Table 1
Symbols, definitions and units for OASIM

Symbol	Definition	Units
λ	Wavelength	nm
λ_m	Wavelength in meters (for calculating PAR)	m
E_d	Direct irradiance at the surface	W m^{-2} (variable spectral width)
E_s	Diffuse irradiance at the surface	W m^{-2} (variable spectral width)
cov	Cloud cover	Percent
F_o	Extraterrestrial irradiance	W m^{-2} (variable spectral width)
Θ	Solar zenith angle	Degrees
T_g	Transmittance after absorption by atmospheric gases (ozone, oxygen, carbon dioxide, water vapor)	Dimensionless
T_d	Direct transmittance accounting for Rayleigh scattering and aerosol scattering and absorption	Dimensionless
T_s	Diffuse transmittance accounting for Rayleigh scattering and aerosol scattering and absorption	dimensionless
ρ_d	Direct surface reflectance	dimensionless
ρ_s	Diffuse surface reflectance	dimensionless
τ_a	Aerosol optical thickness	dimensionless
ω_a	Aerosol single scattering albedo	dimensionless
α	Aerosol asymmetry parameter	dimensionless
F_a	Aerosol forward scattering probability	dimensionless
ε_a	Normalization factor for aerosol data sets	dimensionless
τ_c	Cloud optical thickness	dimensionless
LWP	Cloud liquid water path	g m^{-2}
r_e	Cloud droplet effective radius	μm
a	Cloud coefficient for the Delta–Eddington approximation	m^2 g^{-1}
b	Cloud coefficient for the Delta–Eddington approximation	μm m^2 g^{-1}
ε_c	Normalization factor for cloud data sets	dimensionless
E_T	Total surface irradiance (direct+diffuse components) integrated over the entire OASIM spectral domain	W m^{-2}
h	Planck's constant	J s
c	Speed of light	m s^{-1}
N_A	Avogadro's number	mol^{-1}
PAR	photosynthetically available	mol photons m^{-2} d^{-1}

derive monthly climatologies based on our MODIS τ_a interpolations described above. We normalize climatological OASIM $\tau_a(625)$ to the AVHRR $\tau_a(630)$, and then derive the full OASIM spectral complement from this relationship when only AVHRR aerosols are available

$$\varepsilon_a(\lambda) = \tau_{ac}(\lambda)/\tau_{ac}(625) \quad (7)$$

where τ_{ac} is a monthly climatology. Then

$$\tau_a(\lambda) = \varepsilon_a(\lambda)\tau_{aa} \quad (8)$$

where τ_{aa} is the AVHRR aerosol optical thickness, which is assumed equal to OASIM at 625 nm. We use MODIS climatologies for spectral ω_a and α before Feb 2000. Where neither AVHRR nor MODIS aerosol data are available, we default to the marine aerosol characterization of Gregg and Carder (1990).

Annual trends of OASIM $\tau_a(625)$ for the period 1984–2005 showed a discontinuity in year 2000, corresponding with the change from AVHRR to MODIS τ_a. Global OASIM $\tau_a(625)$ derived from AVHRR was observed to have a bias of −0.025 relative to that derived from MODIS, so we adjust AVHRR τ_a (630) by this amount to remove the bias.

Under cloudy skies, OASIM utilizes the cloudy sky model of Slingo (1989). This model computes irradiance transmittance through clouds spectrally using a Delta–Eddington approximation of the two-stream approach. In our implementation of the Slingo (1989) model, gaseous absorption by ozone, oxygen, carbon dioxide, and water vapor occurs before cloud transmittance, and Rayleigh and aerosol effects are ignored in the presence of clouds. The Slingo model requires 4 cloud properties: cloud cover, cloud liquid water path (ice clouds are ignored in OASIM), cloud optical thickness, and cloud droplet effective radius (symbols and definitions are shown in Table 1). Any one of the latter three can be determined from the other two, using

$$\tau_c = \mathrm{LWP}[a(\lambda) + b(\lambda)/r_e] \quad (9)$$

(Slingo, 1989). LWP is from ISCCP (Rossow et al., 1996). r_e is produced by MODIS. Unfortunately, initial analyses showed very poor results using MODIS r_e in our model. Kiehl et al. (1998) suggested the mean ocean r_e is 10 μm, while Han et al. (1994) suggested a value of 11.8 μm. We use the mean of these

Table 2
Atmospheric optical data for OASIM

λ	F_o	τ_r	a_{oz}	a_{wv}	a_{o2}	a_{co2}
250	16.5280	2.8229	80.8836	0.0000	0.0000	0.0000
325	41.0035	0.8742	0.3584	0.0000	0.0000	0.0000
350	12.7915	0.5925	0.0016	0.0000	0.0000	0.0000
375	27.1180	0.4768	0.0001	0.0000	0.0000	0.0000
400	35.1935	0.3643	0.0000	0.0000	0.0000	0.0000
425	42.1795	0.2833	0.0008	0.0000	0.0000	0.0000
450	49.1940	0.2238	0.0040	0.0000	0.0000	0.0000
475	49.7700	0.1791	0.0121	0.0000	0.0000	0.0000
500	48.3945	0.1451	0.0279	0.0000	0.0000	0.0000
525	46.4935	0.1189	0.0529	0.0000	0.0000	0.0000
550	46.5160	0.0983	0.0832	0.0000	0.0000	0.0000
575	46.1380	0.0820	0.1140	0.0148	0.0000	0.0000
600	44.1230	0.0690	0.1176	0.0851	0.0000	0.0000
625	42.0468	0.0584	0.0967	0.0016	0.0058	0.0000
650	39.5245	0.0498	0.0643	0.0408	0.0000	0.0000
675	37.8730	0.0427	0.0416	0.0009	0.2333	0.0000
700	18.7465	0.0382	0.0261	0.1074	0.1299	0.0000
725	66.8775	0.0319	0.0132	0.1462	0.0000	0.0000
775	59.9900	0.0244	0.0072	0.0065	1.1176	0.0000
850	102.2358	0.0168	0.0020	0.0568	0.0001	0.0000
950	84.7899	0.0108	0.0000	4.9142	0.0000	0.0000
1050	67.8772	0.0072	0.0000	0.0279	0.0002	0.0002
1150	56.0762	0.0050	0.0000	17.5902	0.0000	0.0000
1250	46.1106	0.0032	0.0000	0.0479	0.0028	0.0005
1350	37.3780	0.0026	0.0000	115.3197	0.0000	0.0003
1450	31.8313	0.0020	0.0000	95.2031	0.0000	0.0023
1550	27.2524	0.0015	0.0000	0.0364	0.0000	0.0014
1650	22.7691	0.0012	0.0000	0.0082	0.0000	0.0010
1750	18.6144	0.0009	0.0000	2.0008	0.0000	0.0001
1900	27.9521	0.0007	0.0000	228.9211	0.0000	0.0087
2200	33.6300	0.0004	0.0000	0.2550	0.0000	0.0118
2900	32.5775	0.0001	0.0000	314.7111	0.0000	0.0256
3700	7.2635	0.0000	0.0000	0.9158	0.0000	0.0003

λ is wavelength (nm), F_o is extraterrestrial irradiance (W m^{-2}), τ_r is Rayleigh optical thickness (dimensionless), a_{oz} is ozone absorption coefficient (cm^{-1}), a_{wv} is water vapor absorption coefficient (cm^{-1}), a_{o2} is oxygen absorption coefficient (cm^{-1}), and a_{co2} is carbon dioxide absorption coefficient (cm^{-1}). A data file is available online at http://gmao.gsfc.nasa.gov/research/oceanbiology/index.php.

Please cite this article as: Gregg, W.W., Casey, N.W., Skill assessment of a spectral ocean–atmosphere radiative model, Journal of Marine Systems (2008), doi:10.1016/j.jmarsys.2008.05.007

two estimates to normalize MODIS r_e data. OASIM r_e is derived from the MODIS r_e values multiplied by a factor ε_c

$$r_e = \varepsilon_c \bar{r}_e \tag{10}$$

$$\varepsilon_c = [(10.0 + 11.8)/2]/\bar{r}_e \tag{11}$$

where 10.0 and 11.8 represent the estimated ocean r_e values (in μm) from Kiehl et al. (1998) and Han et al. (1994), respectively. $\bar{r}_e$ is simply the mean of all MODIS-derived r_e values over the entire OASIM domain for a month. Climatological r_e is used for the time periods preceding MODIS r_e availability.

The spectral and directional effects of clouds are depicted in Fig. 3. Clouds change the amount of irradiance reaching the ocean surface (here about half the clear sky total), and also the directional quality. Most of the irradiance under cloudy skies is diffuse, and there is very little direct reaching the surface. This is in contrast to the clear sky case, where most surface irradiance is direct. There are spectral effects as well, which are difficult to see in Fig. 3: clouds shift irradiance toward the shorter wavelengths by about 20% in this case, at the expense of the longer visible wavelengths (650–700 nm), which are reduced by 9% relative to clear skies.

For both the clear and cloudy sky models, transmittance across the ocean interface employs spectral surface reflectance in the presence of sea foam based on observations by Frouin et al. (1996), and confirmed by Moore et al. (1998). This modification accounts for the fact that some of the reflectance by sea foam is due to bubbles located slightly below the surface. This produces some absorption by sea water before reflecting the light out of the water. Since longer wavelengths are much more strongly absorbing than shorter ones, the net effect is reduction of foam reflectance at longer wavelengths. This treatment is described in the Appendix.

Atmospheric data sets are also required (Table 3). These include cloud properties (cloud cover and liquid water path), as well as surface pressure (for Rayleigh scattering and gaseous absorption by oxygen and carbon dioxide), wind speeds (for foam reflectance and default aerosol characterization), relative humidity (for default aerosol characterization), precipitable water (absorption by water vapor), and ozone (gaseous absorption). Cloud cover and LWP are from ISCCP monthly mean data made available by the NASA/Goddard Institute for Space Studies (Rossow et al., 1996). Surface pressure, wind speeds, relative humidity, precipitable water are from NCEP Reanalysis (Kalnay et al., 1996). Ozone is from the multi-decadal record beginning in 1978 of several Total Ozone Mapping Spectrometer (TOMS) sensors. Aerosol optical thickness is taken from the Advanced Very High Resolution Radiometer (AVHRR) from 1981 to Feb 2000. Aerosol optical thickness data from MODIS (Remer et al., 2005) is used beginning in Mar 2000, from Terra until July 2002, when Aqua was launched, then Terra combined with Aqua thereafter). For single scattering albedo and asymmetry parameter, we also use data from MODIS. Climatologies are used when monthly data were not available.

In principle, OASIM has no space or time resolution limitations. In practice, OASIM is limited by the space/time resolutions available in the required forcing data sets (Table 3). For Earth-mapped data products, the spatial resolution ranges from about 1° (MODIS aerosol and cloud data) to 2.5° (NCEP and ISCCP data). Temporally, the resolutions span the range of 3 h (ISCCP clouds) to monthly (MODIS clouds and aerosols). Finer spatial and temporal resolutions for many of the data sets are available but require substantial computer storage and post-processing. Our standard configuration for OASIM is 1°, and data sets with lower resolution are interpolated to this resolution. We routinely execute OASIM at two-hour intervals throughout the day to capture diurnal variability. In this case the solar zenith angle varies over a field of constant daily atmospheric optical constituents, and is averaged to produce mean

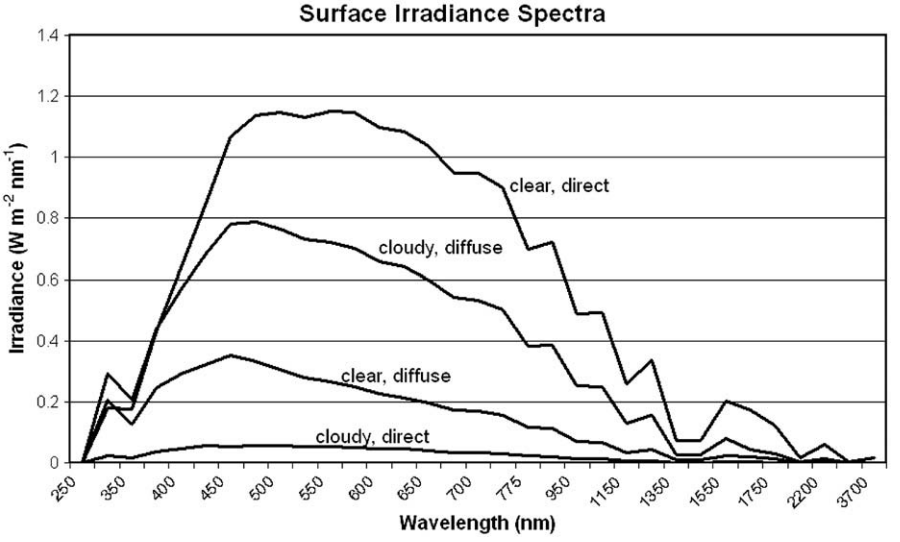

Fig. 3. Spectral surface irradiance just below the sea surface (after spectral surface reflectance) for clear skies and cloudy skies. The cloudy sky simulation represents the effects of 80 g m^{-2} liquid water path, which produces about half the total surface solar irradiance as the clear sky model for the same solar zenith angle and atmospheric optical properties.

Please cite this article as: Gregg, W.W., Casey, N.W., Skill assessment of a spectral ocean–atmosphere radiative model, Journal of Marine Systems (2008), doi:10.1016/j.jmarsys.2008.05.007

Table 3
Data sets needed for OASIM and dates available

	1979	1981/07	1983/06	1993/05	1996/07	2000/03	2002/07
Clouds							
Cover	ISCCP climatology		ISCCP →				
LWP	ISCCP climatology		ISCCP →				
r_e	MODIS climatology →					MODIS-Terra →	MODIS-Terra+Aqua
Aerosols							
τ_a	AVHRR climatology →					MODIS-Terra →	MODIS-Terra+Aqua
ω_a	MODIS climatology →					MODIS-Terra →	MODIS-Terra+Aqua
Asymmetry	MODIS climatology →					MODIS-Terra →	MODIS-Terra+Aqua
Ozone	Nimbus-7 TOMS →			Climatology →	EP-TOMS →		
Sfc Pressure	NCEP →						
Wind Speed	NCEP →						
Rel. humidity	NCEP →						
Precip. water	NCEP →						

ISCCP is the International Satellite Cloud Climatology Project; MODIS is the Moderate Resolution Imaging Spectroradiometer(Terra and Aqua are spacecraft); AVHRR is the Advanced Very High Resolution Radiometer; TOMS is the Total Ozone Mapping Spectrometer (Nimbus-7 and EP (Earth Probe) are spacecraft); and NCEP is the National Center for Environmental Prediction.

monthly values at each 2-hour increment. This standard configuration produces surface spectral irradiance at monthly mean 2-hour intervals just below the sea surface, accounting for surface reflectance. Software is available for public use (see Software and Data Availability section at the end of the paper).

3. Data and skill assessment methods

In situ data sets and publicly available global data products of total surface irradiance and PAR are used to assess the skill of OASIM. All of these comparisons are broadband comparisons, because there is very little data on spectral surface irradiance. We obtained >2000 observations of monthly total surface irradiance from 16 sources (Table 4), distributed globally (Fig. 4). Most of the data sets reported monthly surface irradiance, but a few reported hourly or even finer time scales. In the hourly and finer cases, the reports were required to be continuous over the days and months to be included in our assessment. However, we consider a minor number of missing days to be acceptable, as long as the reports were continuous throughout the day. The data sets are averaged over the month to produce monthly means. The global data products for total irradiance are ISCCP-FD (July 1983–December 2004), NCEP (1984–2004), and ISLSCP II (1986–1995), which are all derived from models. ISCCP and NCEP are 2.5-degree monthly resolution, and ISLSCP II is 1-degree monthly. Comparisons of these global data products (as well as OASIM) with in situ data sets necessarily includes a mis-match in spatial scales. This likely contributes to uncertainty in the comparisons, but is the best representation of the data products at their configured resolutions.

For skill assessment, OASIM is re-configured to produce above-water irradiance, i.e., transmittance through the ocean surface interface (the $[1-\rho_{d,s}(\lambda)]$ terms in Eqs. (1) and (2)) is ignored to conform with the available data products. OASIM spectral irradiance is integrated over the entire solar spectrum (200 nm to 4 μm for total irradiance) and over the direct and diffuse components to produce total surface irradiance, E_T

$$E_T = \int_{200nm}^{4\mu m} [E_d(\lambda) + E_s(\lambda)] d\lambda \quad (12)$$

at each of the 2-hour increments in the standard configuration. These 2-hour increments are averaged over the month and then divided by 12 to produce monthly mean total surface irradiance. Again this produces conformity with the in situ and data products for a meaningful comparison.

SeaWiFS PAR from Sep 1997 to Dec 2004 is used to assess the skill of OASIM over the PAR spectral region. This is a widely used data product derived from the radiances of SeaWiFS, which has shown good agreement with limited in situ data sets (Frouin et al., 2003). PAR is formally defined as

$$\mathrm{PAR} = 1/(hcN_A) \int_0^{24} \int_{350nm}^{700nm} \lambda_m [E_d(\lambda) + E_S(\lambda)] d\lambda dt \quad (13)$$

Eq. (13) strictly applies for OASIM. For SeaWiFS PAR, the spectral integral is from 400–700 nm.

Skill assessment consists of statistical measures of bias, root-mean square (RMS) difference, correlation, and linear regression analysis, specifically slope and intercept of a best-fit regression line. All of the procedures are defined in Stow et al. (this issue), except slope and intercept, which are described in many texts (e.g., Zar, 1974). The RMS is used here as a measure of the total error, i.e., bias and uncertainty (or dispersion) of the model-data comparison. The bias represents the mean departure of the model from the observations. The correlation coefficient shows the ability of the model to represent the spatial and temporal variability shown in the observations. The slope and intercept are important because they show how the model-data errors are distributed across the range of irradiances encountered. For example, a non-unity slope of the best-fit regression line may indicate problems at

Please cite this article as: Gregg, W.W., Casey, N.W., Skill assessment of a spectral ocean–atmosphere radiative model, Journal of Marine Systems (2008), doi:10.1016/j.jmarsys.2008.05.007

Table 4
In situ data sets for total surface irradiance used for comparison with OASIM

Experiment	Lon	Lat	Start	End	*N*	Location	Data set access
ARABSEA Arabian Sea Mixed Layer Dynamics Experiment	61.50	15.50	11/ 1994	9/ 1995	11	Arabian Sea	http://kuvasz.whoi.edu/uopdata/arabiansea/arabiansea.html http://uop.whoi.edu/completedprojects/arabian_sea/os96poster.html
ASREX91 Acoustic Surface Reverberation Experiment	−132.00	49.23	11/ 1991	12/ 1991	2	Eastern North Pacific (off Vancouver)	http://kuvasz.whoi.edu/uopdata/asrex91/asrex91.html
ASREX93 Acoustic Surface Reverberation Experiment	−69.70	33.90	1/ 1994	2/ 1994	2	Western North Atlantic (off Carolinas)	http://kuvasz.whoi.edu/uopdata/asrex93/asrex93.html
BIOWATT Bio-Optical and Physical Moored Measurement Program	~−70.0	~34.0	3/ 1987	10/ 1987	8	Sargasso Sea	http://kuvasz.whoi.edu/uopdata/biowatt/biowatt.html
CMO Coastal Mixing and Optics Moored Array	−70.50	40.49	8/ 1996	5/ 1997	10	South of Cape Cod (New England shelf)	http://kuvasz.whoi.edu/uopdata/cmo/cmo.html http://uop.whoi.edu/completedprojects/cmo/uopcmo.html
COARE Coupled Ocean-Atmosphere Response Experiment	156.0	−1.76	11/ 1992	2/ 1993	4	Western Equatorial Pacific (tropical warmpool)	http://kuvasz.whoi.edu/uopdata/coare/coare.html http://uop.whoi.edu/completedprojects/toga.htm
FASINEX Frontal Air–Sea Interaction Experiment	~−70.0	~27.0	2/ 1986	5/ 1986	4	Southwest of Bermuda	http://kuvasz.whoi.edu/uopdata/fasinex/fasinex.html
MLML 89 Marine Light- Mixed Layers Experiment	−20.83	59.50	5/ 1989	5/ 1989	1	South of Iceland	http://kuvasz.whoi.edu/uopdata/mlml/mlml89/mlml89.html
MLML 91 Marine Light- Mixed Layers Experiment	−21.00	59.50	5/ 1991	8/ 1991	4	South of Iceland	http://kuvasz.whoi.edu/uopdata/mlml/mlml91/mlml91.html
NTAS Northwest Tropical Atlantic Station	-51.00	14.83	4/ 2001	2/ 2002	11	Tropical Atlantic	http://uop.whoi.edu/projects/NTAS/ntas.htm
PMEL Pacific Marine Environmental Laboratory TAO/TRITON/PIRATA	−180 to 180	−10.0 to 15.0	11/ 1991	4/ 2005	2110	Equatorial Pacific and Atlantic	http://www.pmel.noaa.gov/tao/index.shtml http://www.pmel.noaa.gov/tao/data_deliv/deliv.html
SESMOOR Severe Environment Surface Mooring	−61.20	42.50	11/ 1988	2/ 1989	4	Western North Atlantic	http://kuvasz.whoi.edu/uopdata/sesmoor/sesmoor.html
SMILE Shelf Mixed Layer Experiment	−123.49	38.65	12/ 1988	4/ 1989	5	Northern California shelf	http://kuvasz.whoi.edu/uopdata/smile/smile.html
STRATUS 1	−85.15	−20.15	11/ 2000	9/ 2001	11	Eastern Tropical Pacific (off Peru)	http://uop.whoi.edu/projects/Stratus/stratus.htm http://uop.whoi.edu/projects/Stratus/stratusarchive.htm
STRATUS 2	−85.14	−20.14	11/ 2001	9/ 2002	11	Eastern Tropical Pacific (off Peru)	http://uop.whoi.edu/projects/Stratus/stratus.htm http://uop.whoi.edu/projects/Stratus/stratusarchive.htm
SUBDUCTION	5 sites		7/ 1991	5/ 1993	115	West of Africa	http://kuvasz.whoi.edu/uopdata/subduction/subduction.html
WHOTS Hawaii Ocean Time-series Station	~−158.0	~22.75	10/ 2004	6/ 2005	9	Hawaii	http://uop.whoi.edu/projects/WHOTS/whots.htm

All data sets are from the Woods Hole Oceanographic Institution–Upper Ocean Processes Group (WHOI–UOP) except for PMEL (TAO: Tropical Atmosphere Ocean project; TRITON: Triangle Trans-Ocean Buoy Network; PIRATA: Pilot Research Moored Array in the Atlantic).

high or low irradiances, which can be associated with cloudy or clear skies. Together with the other statistical metrics, they provide useful information on the distribution of the errors over the range. Additionally we provide two-dimensional image representations of OASIM and model data products, along with difference fields.

4. Results and discussion

4.1. Total surface irradiance

OASIM total surface irradiance compared with 2322 in situ observations yielded RMS = 20.1 W m^{-2}, bias = 1.6 W m^{-2}, with regression slope = 1.01 and correlation coefficient = 0.89 (Fig. 5). These statistics suggest good correspondence with observations. The low bias and near unity regression slope are particularly noteworthy. Considering a global annual mean of 188.0 W m^{-2}, the RMS represents a total error of about 11%, and bias about 0.8%. OASIM had the lowest bias of any of the other data products evaluated (ISCCP-FD, NCEP and ISLSCP II; Fig. 5), and the best slope (nearest to unity). OASIM had the second best RMS, (ISCCP-FD was better at 19.0 W m^{-2}, or about 10%), and the third best correlation coefficient, (ISCCP-FD at 0.932 and ISCSCP II at 0.97 were better). NCEP performed the worst of the 4 data products in terms of RMS (29.8 W m^{-2}), correlation coefficient (0.7) and regression

Please cite this article as: Gregg, W.W., Casey, N.W., Skill assessment of a spectral ocean–atmosphere radiative model, Journal of Marine Systems (2008), doi:10.1016/j.jmarsys.2008.05.007

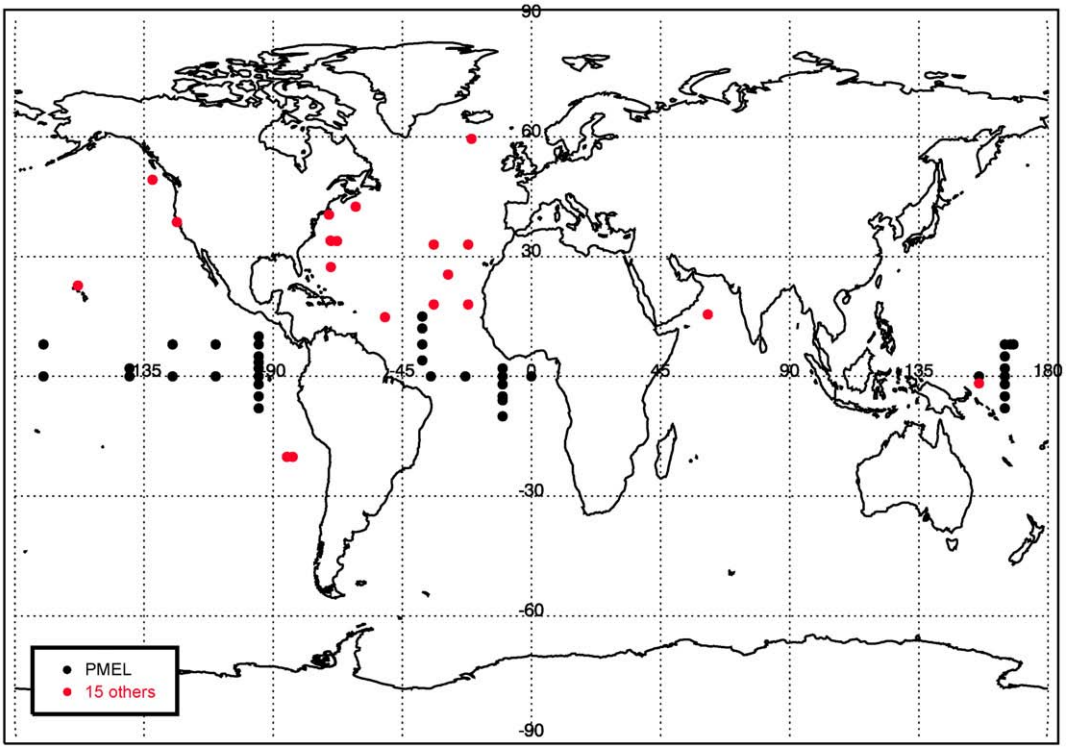

Fig. 4. Distribution of in situ observations of total surface irradiance.

slope (0.6). It had low bias, however (7.5 W m^{-2}, or about 4%). This illustrates the importance of slope in skill assessment. NCEP's low bias was the result of compensating errors at the low and high end of the irradiance range. The low slope clearly shows why the low bias is misleading in this case. ISLSCP II had the highest correlation coefficient, but also the highest bias (17.7 W m^{-2}). Scatterplots of each of the data sets against in situ observations (Fig. 6) reinforced the statistics. Note that ISLSCP II had far fewer matchups with observations than OASIM, ISCCP-FD, and NCEP because of the shorter duration of the data product.

The low bias of OASIM has important implications for ocean biological models and primary production algorithms because it suggests a more globally representative estimate of downwelling surface irradiance, potentially leading to improved estimates of large-scale biological variables and

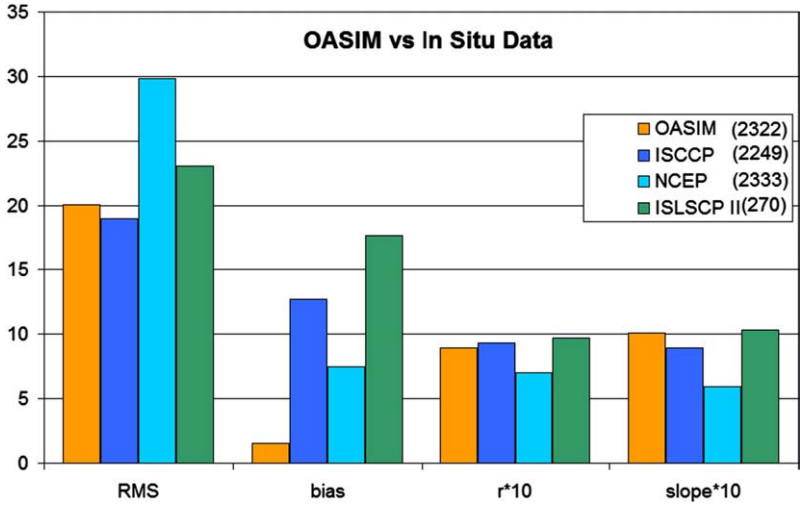

Fig. 5. Statistics on the comparison between OASIM, ISCCP, NCEP, and ISLSCP II and in situ total surface irradiance observations. Note that correlation coefficient r and slope are multiplied by 10. The number of comparisons with in situ data are shown in the legend. The first 2 metrics, RMS and bias, are best if closer to 0, the last two, r and slope, are best if closer to 1 (or 10 in this plot according to the scaling factor used).

Please cite this article as: Gregg, W.W., Casey, N.W., Skill assessment of a spectral ocean–atmosphere radiative model, Journal of Marine Systems (2008), doi:10.1016/j.jmarsys.2008.05.007

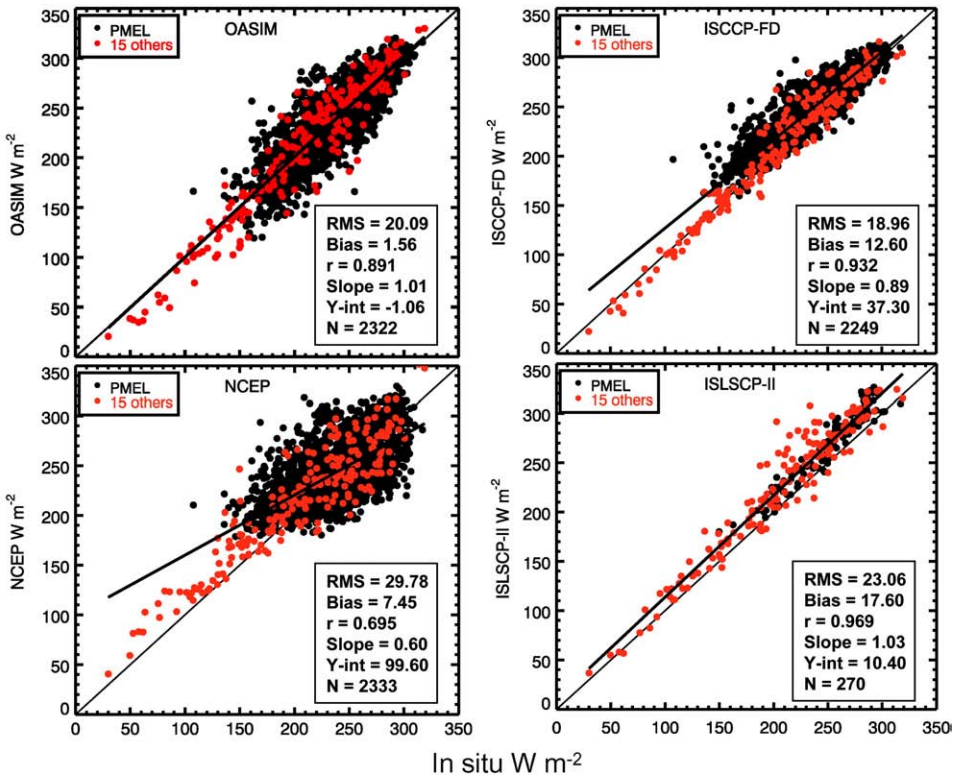

Fig. 6. Scatterplots of the relationships between global data products and in situ total irradiances.

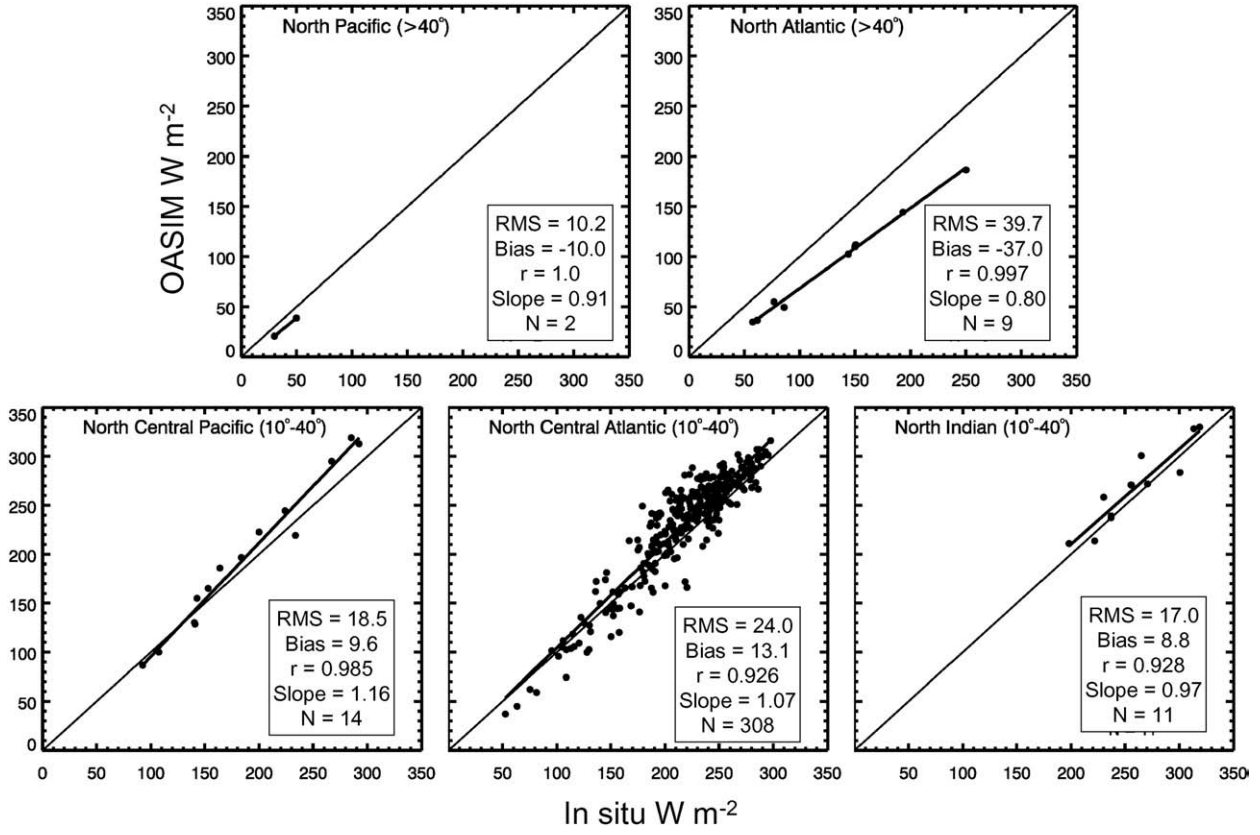

Fig. 7. Scatterplots of the relationships between OASIM and in situ total irradiances for northern oceanographic basins, including statistics.

Please cite this article as: Gregg, W.W., Casey, N.W., Skill assessment of a spectral ocean–atmosphere radiative model, Journal of Marine Systems (2008), doi:10.1016/j.jmarsys.2008.05.007

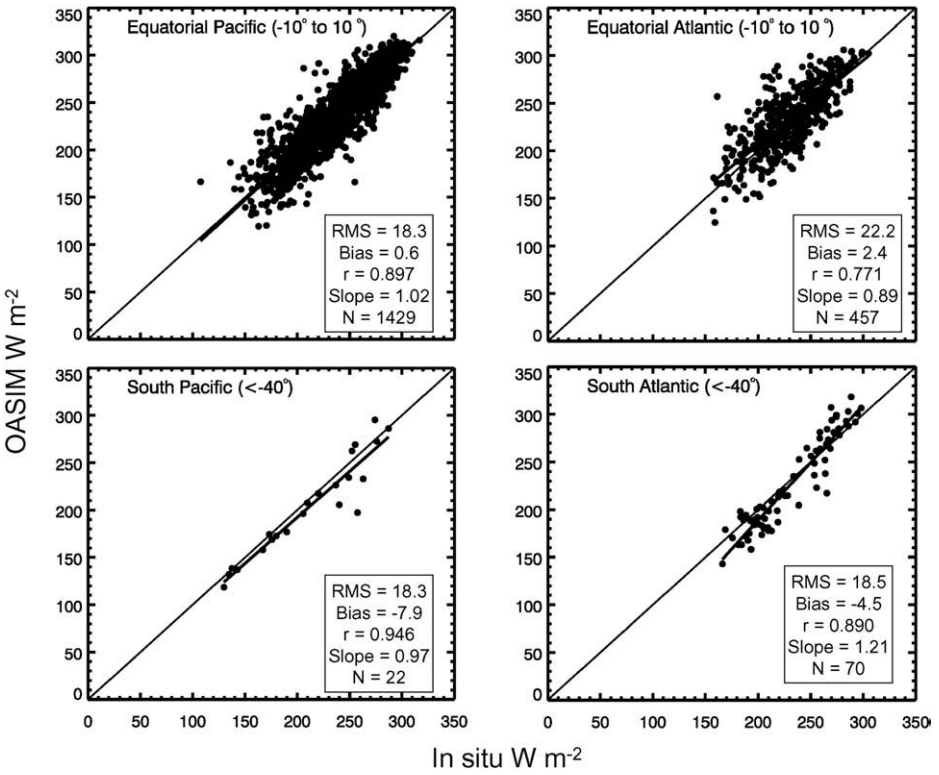

Fig. 8. Scatterplots of OASIM and in situ total irradiances for equatorial and southern oceanographic basins.

fluxes. The near unity slope indicates that OASIM matches surface irradiance across the entire range of irradiances, from 20 to nearly 350 W m^{-2}. Although the total error as represented by RMS was not as good as ISCCP-FD (the best of the global data products), it differed by only 1.1 W m^{-2}.

A regional comparison of OASIM with surface data sets is difficult because the in situ data are not distributed in all of the major ocean basins, and only sparsely in some. However, it can provide some indication of its performance. The equatorial basins were the most heavily sampled, and here OASIM compared favorably with data (Figs. 7 and 8). Similar encouraging statistics were observed in the remainder of basins sampled, except the North Atlantic. Although caution is needed in interpreting the statistics here because there were only 9 observations, a clear low bias was apparent in OASIM. There were only 2 observations in the North Pacific, so the statistics should be considered with even more caution (correlation coefficient is completely meaningless). However, the 2 observations indicated that the poor results in the North Atlantic were not replicated here.

When compared directly with the global data products, OASIM total surface irradiance tracked well with ISCCP-FD (RMS = 20.7 W m^{-2}; bias = −11.4 W m^{-2}, r = 0.98) and also ISLSCP II (RMS = 25.2 W m^{-2}; bias = −13.8 W m^{-2}; r = 0.97), but less well with NCEP (RMS = 43.0 W m^{-2}; bias = −22.6 W m^{-2}; r = 0.91) (Table 5). Note that OASIM bias was always negative, indicating that OASIM provided the lowest estimates of total surface irradiance. The near unity slope of OASIM vs. the other data products was apparent, but there was considerable uncertainty (RMS) in the comparison with NCEP. Considering that ISCCP-FD, ISLSCP II, and OASIM all use ISCCP cloud data (although ISCCP and ISLSCP II use cloud optical thickness while OASIM uses cloud liquid water path), the agreement among these three data products is not surprising.

Global distributions of the total surface downwelling irradiance and difference fields illustrated the similarities and differences between OASIM and the global data products for March 1990 (Fig. 9), a typical month. The spatial structure was very similar between OASIM and ISCCP and OASIM and ISLSCP II. However, OASIM estimated lower irradiance where irradiance was moderate-to-low, and higher where irradiances were high. The spatial structure of OASIM was in

Table 5
Statistics on the comparison of OASIM with other global data products

	ISCCP-FD	NCEP	ISLSCP-II
Slope	1.02	1.03	1.02
Correlation coefficient	0.980	0.907	0.969
RMS	20.67	42.99	25.15
Bias	−11.41	−22.64	−13.82
N	8.6×10^6	8.6×10^6	4.0×10^6

RMS and bias are in units of W m^{-2}.

Please cite this article as: Gregg, W.W., Casey, N.W., Skill assessment of a spectral ocean–atmosphere radiative model, Journal of Marine Systems (2008), doi:10.1016/j.jmarsys.2008.05.007

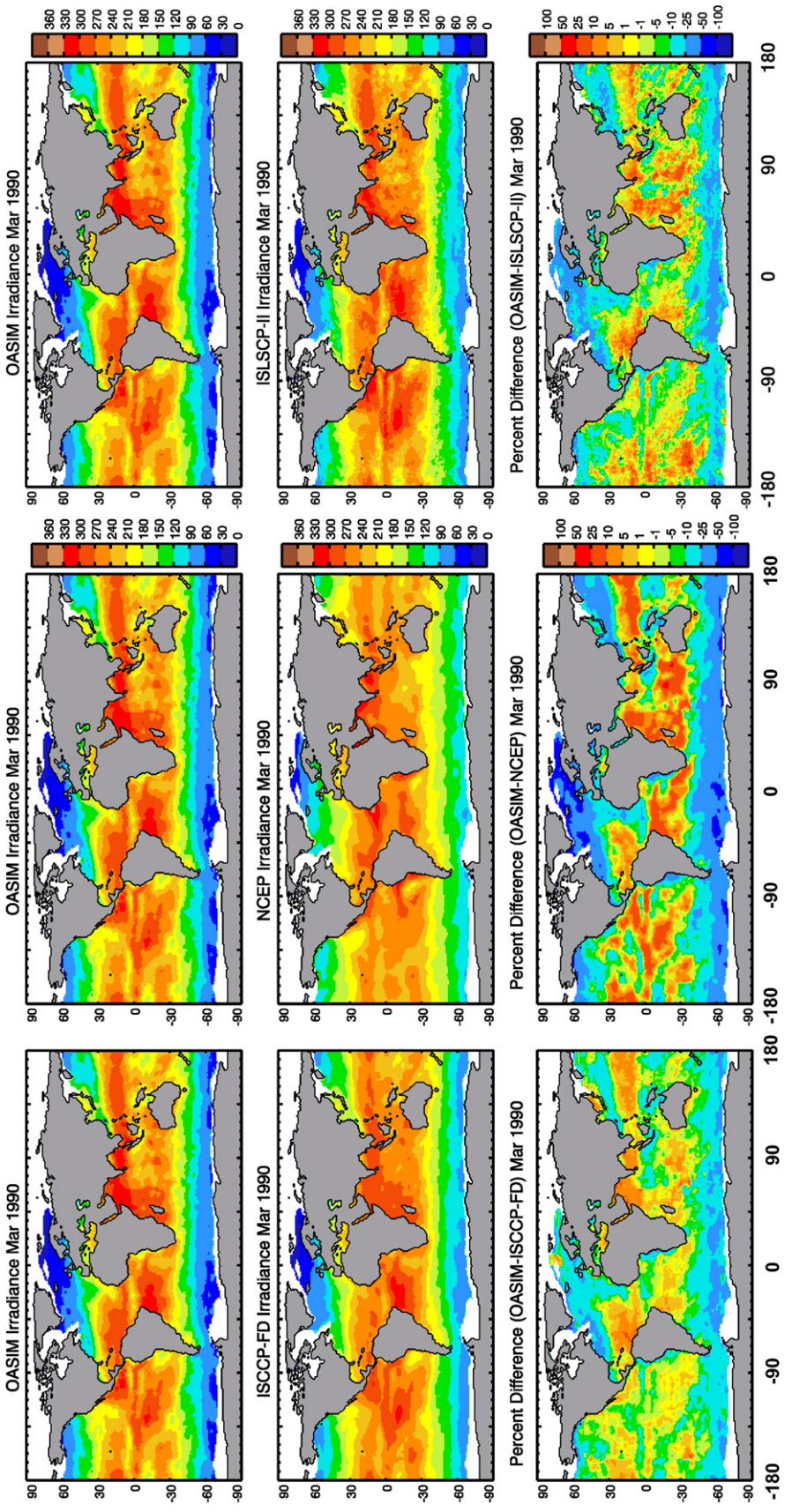

Fig. 9. Global distributions of estimated total surface downwelling irradiance for OASIM, ISCCP, NCEP, and ISLSCP II for March 1990. Difference fields (OASIM–global data set) are shown.

Please cite this article as: Gregg, W.W., Casey, N.W., Skill assessment of a spectral ocean–atmosphere radiative model, Journal of Marine Systems (2008), doi:10.1016/j.jmarsys.2008.05.007

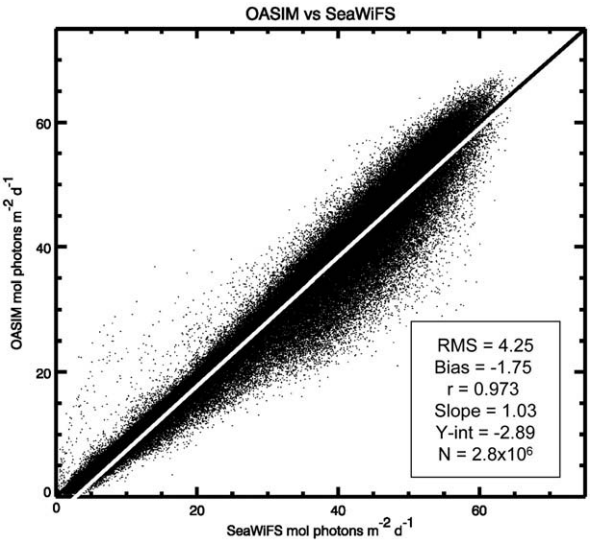

Fig. 10. Scatterplot of the comparison between OASIM PAR and SeaWiFS PAR. Statistics are shown.

very broad agreement with NCEP (as reflected in the correlation coefficient), but there were many differences in magnitude and fine structure (as reflected in the RMS and bias).

4.2. PAR

Comparison of OASIM PAR with SeaWiFS PAR showed excellent correspondence (Fig. 10). Low bias (−1.8 mol photons m^{-2} d^{-1}, or about 5% on a background of 36 mol photons m^{-2} d^{-1} for an annual mean), RMS (4.25 mol photons m^{-2} d^{-1}, or about 12%), near unity slope (1.03) and high correlation coefficient (0.973) characterized the statistical comparison. There was considerable scatter in the relationship among a small number of coincident values at the low end of the PAR range, while most of the uncertainty resided toward the middle of the range. Global distributions of PAR (Fig. 11) and the difference fields showed overall agreement, but also regions of divergence. OASIM tended to be higher than SeaWiFS in regions of high PAR. OASIM produced lower estimates in the tropics and the eastern Pacific.

The SeaWiFS PAR product was previously compared to observations at two stations, Halibut Banks off British Columbia, Canada, and the tropical Pacific (Frouin et al., 2003). Overall, the results were quite good for monthly means (RMS=3.3 mol photons m^{-2} d^{-1}; bias=2.2 mol photons m^{-2} d^{-1}, r=0.989; Frouin et al., 2003). One of the most important drawbacks in the SeaWiFS PAR product is the lack of diurnal variability in clouds, due to the use of a single sensor in a near-noon orbit. The lower correlation coefficient in the Equatorial Pacific (0.820) compared to Halibut Banks (0.997) suggests that SeaWiFS PAR may miss afternoon clouds. OASIM uses monthly mean ISCCP clouds, which are derived from 3-hourly observations in mid-latitudes, and therefore captures diurnal variability in cloud formation. This probably explains the lower estimates of PAR in the tropics retrieved by OASIM, which is likely more representative.

5. Summary

OASIM total surface irradiance exhibited considerable skill in a comparison with an extensive collection of in situ data as well as global data products from ISCCP-FD, NCEP, and ISLSCP II. It also compared favorably with satellite data products of PAR. These results can be combined with low RMS derived from a validation of the visible spectral clear sky portion of OASIM in a previous study (Gregg and Carder, 1990), which compared within +6.6% RMS with surface observations of spectral irradiance (at 1 nm resolution) and +5.1% RMS with integrated spectral irradiance over the PAR region. Summarizing, the skill assessment of OASIM to date includes global monthly mean total surface irradiance, global monthly spectrally integrated clear sky PAR (spectral range 350–700 nm), and instantaneous spectral visible clear sky surface irradiance (spectral range 350–700 nm). While these results encompass much of the possible skill assessment of OASIM, they are not complete. Unvalidated aspects of OASIM include 200–350 nm and 700 nm to 4 μm under clear skies, and the entire spectral range under cloudy skies. Nevertheless, the fact that OASIM compares favorably with broadband and spectral surface irradiance estimates is encouraging.

6. Software and data product availability

Data products of spectral downwelling irradiance just below the sea surface are available for the period 1979–2005 at http://gmao.gsfc.nasa.gov/research/oceanbiology. The data products are 1° spatial resolution and include direct and diffuse components, each with the 33-band spectral resolution shown in Table 2. The data are also

Please cite this article as: Gregg, W.W., Casey, N.W., Skill assessment of a spectral ocean–atmosphere radiative model, Journal of Marine Systems (2008), doi:10.1016/j.jmarsys.2008.05.007

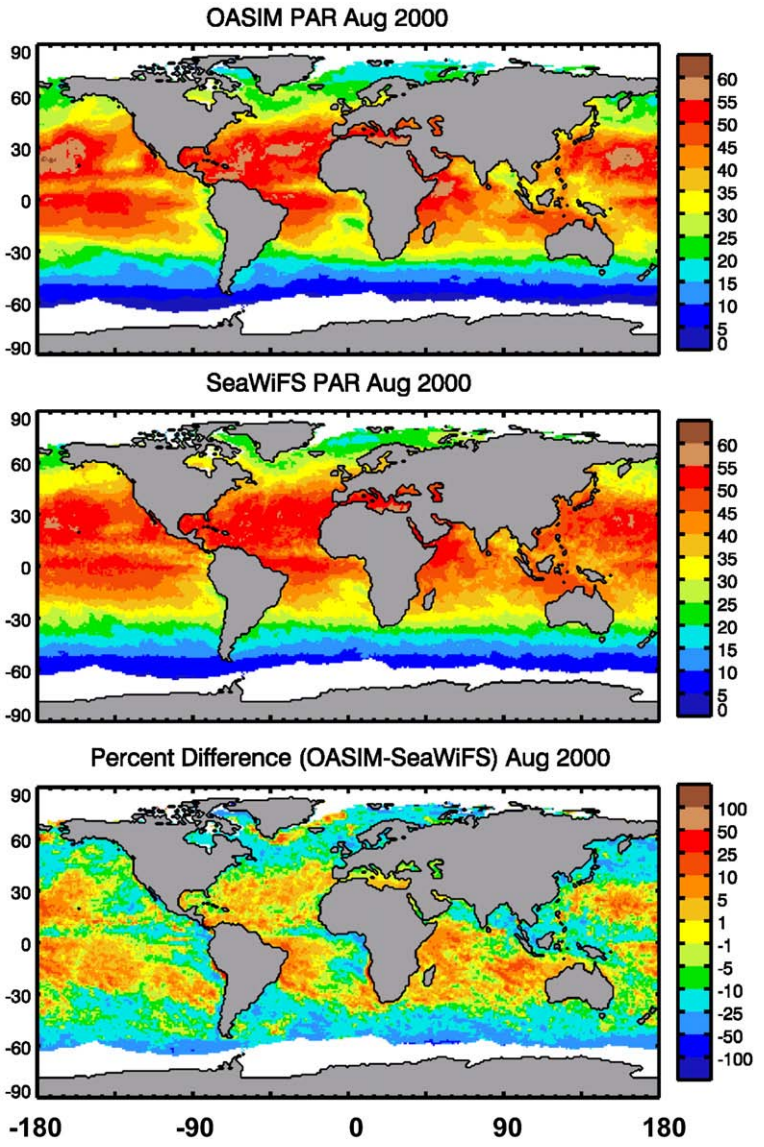

Fig. 11. Global distribution of surface PAR from OASIM and SeaWiFS for August 2000. Units are mol photons m^{-2} d^{-1}. Bottom: difference field OASIM-SeaWIFS.

corrected for transmittance through the ocean interface. Software (Fortran code) for applying OASIM for higher spatial/temporal resolution problems is also available at the same location, but is unsupported.

Acknowledgements

We thank NCEP, ISCCP, ISLSCP, and the NASA Ocean Color Processing team for making surface irradiance and PAR data available. We also thank Michael King and Steven Platnick, NASA/GSFC, for assistance with MODIS cloud data, and Lorraine Remer, NASA/GSFC, for assistance with MODIS aerosol data. In situ data set providers listed in Table 4 are gratefully acknowledged for acquiring these invaluable data sets and making them available. We also thank the providers of atmospheric data, including NCEP, ISCCP, the TOMS Project, AVHRR Pathfinder, and the MODIS cloud and aerosol teams, and the GES-DISC for making these data sets available. Two anonymous reviewers and William B. Rossow, CREST at the City College of New York, provided important suggestions. Support for this work was received from the NASA EOS – and MAP programs (to WWG), and the Ocean Biology and Biogeochemistry program (specifically the Southern Ocean announcement, to Carlos Del Castillo).

Appendix A

A.1 . Calculation of transmittance terms

The transmittance terms in Eqs.(1) and (2) represent absorption by atmospheric gases, $T_g(\lambda)$ and direct and diffuse

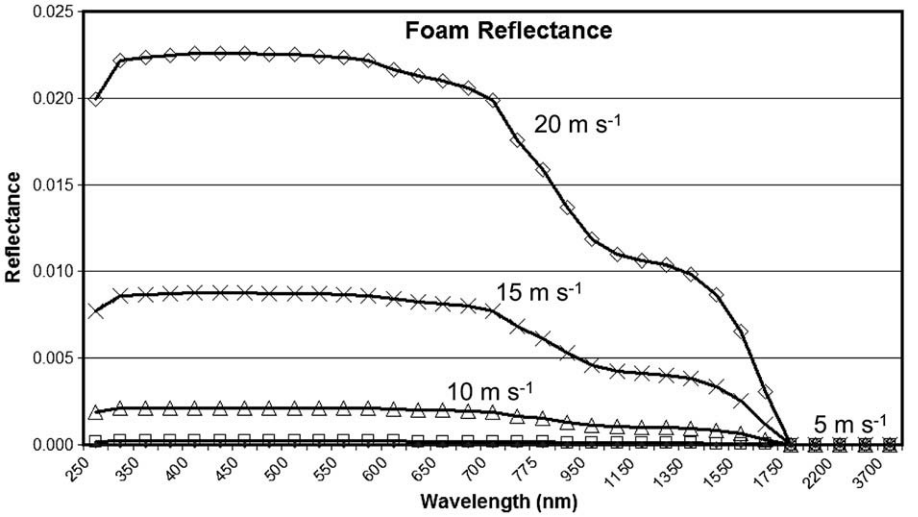

Fig. A.1. Spectral foam reflectance as a function of wind speed.

transmittance due to molecules (Rayleigh scattering), aerosols, and clouds. $T_g(\lambda)$ is common to both the clear and cloudy sky models

$$T_g(\lambda) = T_{oz}(\lambda)T_{oc}(\lambda)T_{wv}(\lambda) \quad \text{(A1)}$$

where T_{oz} is the transmittance due to ozone absorption, T_{oc} is due to oxygen and carbon dioxide absorption, and T_{wv} is due to water vapor (precipitable water) absorption. The transmittance expression for the different atmospheric gases is described in both Bird and Riordan (1986) and Gregg and Carder (1990) and is not defined further here.

A.1.1. Clear sky

Clear sky transmittance arises from the scattering effects of molecules and the scattering and absorbing properties of aerosols

$$T_{dclr}(\lambda) = T_r(\lambda)T_a(\lambda) \quad \text{(A2)}$$

where T_r is the transmittance due to Rayleigh scattering and T_a is that due to aerosol scattering and absorption

$$T_r(\lambda) = \exp[-\tau_r(\lambda)M'(\theta)] \quad \text{(A3)}$$

$$T_a(\lambda) = \exp[-\tau_a(\lambda)M(\theta)] \quad \text{(A4)}$$

where τ_r and τ_a are the Rayleigh and aerosol optical thicknesses, respectively, $M(\theta)$ is the atmospheric path length (see Gregg and Carder, 1990)

$$M(\theta) = 1/\left[\cos\theta\ 0.15(93.885-\theta)^{-1.253}\right] \quad \text{(A5)}$$

and $M'(\theta)$ is the pressure-corrected atmospheric path length

$$M'(\theta) = M(\theta)P/P_0 \quad \text{(A6)}$$

where P is the atmospheric pressure and P_o is standard pressure.

The diffuse transmittance is

$$T_{sclr}(\lambda) = T_{aa}(\lambda)0.5\left(1-T_r(\lambda)^{0.95}\right) + T_r(\lambda)^{1.5}T_{aa}(\lambda)F_a(\lambda)[1-T_{as}(\lambda)] \quad \text{(A7)}$$

where T_{aa} represents the transmittance after aerosol absorption only (not scattering)

$$T_{aa}(\lambda) = \exp\{-[1-\omega_a(\lambda)]\tau_a(\lambda)M(\theta)\} \quad \text{(A8)}$$

and T_{as} represents transmittance due to aerosol scattering only

$$T_{as}(\lambda) = \exp[-\omega_a(\lambda)\tau_a(\lambda)M(\theta)] \quad \text{(A9)}$$

τ_a, ω_a, are taken from satellite data as described in Section 3, and F_a is derived from the satellite-derived asymmetry parameter as described in Eqs. (3)–(6).

A.1.2. Cloudy sky

Rayleigh scattering, and aerosol scattering and absorption are ignored in the cloudy sky model. The cloudy direct and diffuse components, $T_{dcld}(\lambda)$ and $T_{scld}(\lambda)$ are taken from Slingo's (1989) Delta–Eddington approximation. The formulation is described in detail in Slingo (1989) and is not repeated here.

A.2. Calculation of surface reflectance including foam

Frouin et al. (1996) found spectral dependence of foam reflectance, which they attributed to the physical nature of foam: it is composed of air bubbles above the surface separated by a thin layer of water, but also air bubbles submerged just beneath the water. Thus water transmittance plays a role in foam reflectance. Considering these observations by Frouin et al. (1996), foam reflectance is treated as

$$F(\lambda) = a_0 + a_1\ln[T_w(\lambda)] + a_2\ln[T_w(\lambda)]^2 + a_3\ln[T_w(\lambda)]^3;\ \lambda<900\text{nm} \quad \text{(A10)}$$

where F is a factor to adjust foam reflectance for spectral dependence, λ is wavelength in nm, T_w is the transmittance of water

$$T_w(\lambda) = \exp\{-[a_w(\lambda) + 0.5b_w(\lambda)]\} \quad \text{(A11)}$$

Please cite this article as: Gregg, W.W., Casey, N.W., Skill assessment of a spectral ocean–atmosphere radiative model, Journal of Marine Systems (2008), doi:10.1016/j.jmarsys.2008.05.007

where a_w and b_w are the spectral absorption and scattering coefficients of seawater, respectively. The 0.5 factor for b_w represents the backscattered portion. In Eq. (A10), a_0, a_1, a_2, and a_3 are empirical coefficients to produce a best fit to the published data of Frouin et al. (1996), and are 0.9976, 0.2194, 0.0554, and 0.0067, respectively.

At and above 900 nm, a_w is nearly completely absorbing, and a new parameterization is used

$$F(\lambda) = b_0 + b_1\lambda + b_2\lambda^2 + b_3\lambda^3 \; ; \; \lambda \geq 900\text{nm} \qquad \text{(A12)}$$

where b_0, b_1, b_2, and b_3 are defined similarly to their counterparts in Eq. (A10), and are 5.026,−0.0114, 9.552×10^{-6}, and -2.698×10^{-9}, respectively.

Foam reflectance ρ_f now includes spectral dependence through

$$\rho_f(W,\lambda) = \rho_f(W)F(\lambda) \qquad \text{(A13)}$$

where W is the wind speed ($m\ s^{-1}$) and $\rho_f(W)$ is defined as in Gregg and Carder (1990). Surface reflectance is the sum of the specular and foam contributions

$$\rho_d(W,\lambda) = \rho_{dsp}(W) + \rho_f(W,\lambda) \qquad \text{(A14)}$$

$$\rho_s(W,\lambda) = \rho_{ssp}(W) + \rho_f(W,\lambda) \qquad \text{(A15)}$$

where ρ_d and ρ_s represent the direct and diffuse surface reflectance components, and the subscript sp represents specular reflectance (Gregg and Carder, 1990). The relationship between wind speed and foam reflectance is shown for some representative conditions in Fig. A.1.

References

Ahn, Y.-H., Bricaud, A., Morel, A., 1992. Light backscattering efficiency and related properties of some phytoplankters. Deep-Sea Research 39, 1835–1855.

Bartlett, J.S., Ciotti, A.M., Davis, R.F., Cullen, J.J., 1998. The spectral effects of clouds on solar irradiance. Journal of Geophysical Research 103, 31017–31031.

Bird, R.E., Riordan, C., 1986. Simple solar spectral model for direct and diffuse irradiance on horizontal and tilted planes at the Earth's surface for cloudless atmospheres. Journal of Climate and Applied Meteorology 25, 87–97.

Bouvet, M., Hoepfner, N., Dowell, M.D., 2002. Parameterization of a spectral solar irradiance model for the global ocean using multiple satellite sensors. Journal of Geophysical Research 107, C12. doi:10.1029/2001JC001126.

Bricaud, A., Morel, A., Prieur, L., 1983. Optical efficiency factors of some phytoplankton. Limnology and Oceanography 28, 816–832.

Bricaud, A., Bedhomme, A.-L., Morel, A., 1988. Optical properties of diverse phytoplanktonic species: experimental results and theoretical interpretation. Journal of Plankton Research 10, 851–873.

Carr, M.-E., Freidrichs, M.A.M., Schmeltz, M., Aita, M.N., Antoine, D., Arrigo, K.R., Asanuma, I., Aumont, O., Barber, R., Behrenfeld, M., Bidigare, R., Buitenhuis, E., Campbell, J.S., Ciotti, A., Dierssen, H., Dowell, M., Dunne, J., Esaias, W., Gentili, B., Gregg, W., Groom, S., Hoepffner, N., Ishizaka, J., Kameda, T., LeQuere, C., Lohrenz, S., Marra, J., Melin, F., Moore, K., Morel, A., Reddy, T., Ryan, J., Scardi, M., Smyth, T., Turpie, K., Tilstone, G., Waters, K., Yamanaka, Y., 2006. A comparison of global estimates of marine primary production from ocean color. Deep-Sea Research II 53, 741–770.

Circio, J.A., Petty, C.C., 1951. The near infrared absorption spectrum of liquid water. Journal of the Optical Society of America 41, 302–308.

Frouin, R., Schwindling, M., Deschamps, P.-Y., 1996. Spectral reflectance of sea foam in the visible and near-infrared; in situ measurements and remote sensing implications. Journal of Geophysical Research 101, 14361–14371.

Frouin, R., Franz, B.A., Werdell, P.J., 2003. The SeaWiFS PAR product. In: Hooker, S.B., Firestone, E.R. (Eds.), Algorithm Updates for the Fourth SeaWiFS Data Reprocessing, pp. 46–50. NASA/TM-2003-206892, 22.

Gregg, W.W., Carder, K.L., 1990. A simple spectral solar irradiance model for cloudless maritime atmospheres. Limnology and Oceanography 35, 1657–1675.

Gregg, W.W., Casey, N.W., 2007. Modeling coccolithophores in the global oceans. Deep-Sea Research II 54, 447–477.

Gregg, W.W., Ginoux, P., Schopf, P.S., Casey, N.W., 2003. Phytoplankton and iron: validation of a global three-dimensional ocean biogeochemical model. Deep-Sea Research II 50, 3143–3169.

Hall, F.G., Collatz, G., Los, S., Brown de Colstoun, E., Landis, D. (Eds.), 2005. ISLSCP Initiative II. NASA. DVD/CD-ROM. NASA.

Halthore, R.N., Crisp, D., Schwartz, S.E., Anderson, G.P., Berk, A., Bonnel, B., Boucher, O., Chang, F.-L., Chou, M.-D., Clothiaux, E.E., Dubiosson, P., Fomin, B., Fouquart, Y., Freideneich, S., Gautier, C., Kato, S., Laszlo, I., Li, Z., Mather, J.H., Plana-Fattori, A., Ramaswamy, V., Ricchiazzi, P., Shiren, Y., Trishchenko, A., Wiscombe, W., 2005. Intercomparison of shortwave radiative transfer codes and measurements. Journal of Geophysical Research 110, D11206. doi:10.1029/2004JD005293.

Han, Q., Rossow, W.B., Lacis, A.A., 1994. Near-global survey of effective droplet radii in liquid water clouds using ISCCP data. Journal of Climate 7, 465–497.

Inn, E.C.Y., Tanaka, Y., 1953. Absorption coefficient of ozone in the ultraviolet and visible regions. Journal of the Optical Society of America 43, 870–873.

Kalnay, E., Kanamitsu, M., Kistler, R., Collins, W., Deaven, D., Gandin, L., Iredell, M., Saha, S., White, G., Woollen, J., Zhu, Y., Chelliah, M., Ebisuzaki, W., Higgins, W., Janowiak, J., Mo, K.C., Ropelewski, C., Wang, J., Leetmaa, A., Reynolds, R., Jenne, R., Joseph, D., 1996. The NCEP/NCAR 40-year reanalysis project. Bulletin of the American Meteorological Society 77, 437–471.

Kiehl, J.T., Hack, J.J., Bonan, G.B., Boville, B.A., Williamson, D.L., Rasch, P.J., 1998. The National Center for Atmospheric Research Community climate model: CCM3. Journal of Climate 11, 1131–1149.

Maul, G.A., 1985. Introduction to satellite oceanography. Martinus Nijhoff Publishers, Boston, MA, USA. 606 pp.

Moore, K.R., Voss, K.J., Gordon, H.R., 1998. Spectral reflectance of whitecaps: instrumentation, calibration, and performance in coastal waters. Journal of Atmospheric and Oceanic Technology 15, 496–509.

Morel, A., 1988. Optical modeling of the upper ocean in relation to its biogenous matter content (Case I waters). Journal of Geophysical Research 93, 10749–10768.

Morel, A., Bricaud, A., 1981. Theoretical results concerning light absorption in a discrete medium, and application to specific absorption of phytoplankton. Deep-Sea Research 28, 1375–1393.

Neckel, H., Labs, D., 1984. The solar radiation between 3300 and 12,500 A. Solar Physics 90, 205–258.

Pope, R.M., Fry, E.S., 1997. Absorption spectrum (380–700 nm) of pure water. II. Integrating cavity measurements. Applied Optics 46, 8710–8723.

Remer, L.A., Kaufman, Y.J., Tanre, D., Mattoo, S., Chu, D.A., Martins, J.V., Li, R.-R., Ichoku, C., Levy, R.C., Kleidman, R.G., Eck, T.F., Vermote, E., Holben, B.N., 2005. The MODIS aerosol algorithm, products and validation. Journal of the Atmospheric Sciences 62, 947–973.

Rossow, W.B., Walker, A.W., Beuschel, D.E., Roiter, M.D., 1996. International Satellite Cloud Climatology Project (ISCCP): Documentation of new cloud datasets. World Climate Research Programme, Geneva. WMO/TD- 737, 155 pp.

Sathyendranath, S., Lazzara, L., Prieur, L., 1987. Variations in the spectral values of specific absorption of phytoplankton. Limnology and Oceanography 32, 403–415.

Siegel, D.A., Westberry, T.K., Ohlmann, J.C., 1999. Cloud color and ocean radiant heating. Journal of Climate 12, 1101–1116.

Slingo, A., 1989. A GCM parameterization for the shortwave radiative properties of water cloud. Journal of Atmospheric Sciences 46, 1419–1427.

Smith, R.C., Baker, K.S., 1981. Optical properties of the clearest natural waters (200–800 nm). Applied Optics 20, 177–184.

Stow, C.A., Jolliff, J., McGillicuddy, D.J., Doney, S.C., Allen, J.I., Friedrichs, M.A.M., Rose, K.A., Wallhead, P., 2007. Skill assessment for coupled biological/physical models of marine systems. Journal of Marine Systems, this issue.

Stowe, L., Jacobowitz, H., Ohring, G., Knapp, K., Nalli, N., 2002. The AVHRR Pathfinder Atmosphere (PATMOS) climate data set: initial analyses and evaluation. Journal of Climate 15, 1243–1260.

Tanre, D., Deroo, D., Duhaut, D., Herman, M., Morcrette, J.J., Perbos, J., Deschamps, P.–Y., 1990. Description of a computer code to simulate the satellite signal in the solar spectrum — the 5S code. International Journal of Remote Sensing 11, 659–668.

Thekaekara, M.P., 1974. Extraterrestrial solar spectrum, 3000–6100 A at 1-A intervals. Applied Optics 13, 518–522.

Yang, S., Ricchiazzi, P., Gautier, C., 1999. Modified correlated *k*-distribution methods for remote sensing applications. Journal of Quantitative Spectroscopy and Radiative Transfer 64, 585–608.

Zar, J.H., 1974. Biostatistical analysis. Prentice-Hal, Inc., Englewood Cliffs N.J, USA. 620 pp.

Zhang, Y., Rossow, W.B., Lacis, A.A., Oinas, V., Mischenko, M.I., 2004. Calculation of radiative fluxes from the surface to top of atmosphere based on ISCCP and other global data sets: refinements of the radiative transfer model and input data. Journal of Geophysical Research 109, D19105. doi:10.1029/2003JD004457.

Please cite this article as: Gregg, W.W., Casey, N.W., Skill assessment of a spectral ocean–atmosphere radiative model, Journal of Marine Systems (2008), doi:10.1016/j.jmarsys.2008.05.007